On the Design of Orthogonal Pulse-Shape Modulation for UWB Systems Using Hermite Pulses

Giuseppe Thadeu Freitas de Abreu, Craig John Mitchell, and Ryuji Kohno

Abstract: **Orthogonal pulse-shape modulation using Hermite pulses for ultra-wideband communications is reviewed. Closed-form expressions of cross-correlations among Hermite pulses and their corresponding transmit and receive waveforms are provided. These show that the pulses lose orthogonality at the receiver in the presence of differentiating antennas. Using these expressions, an algebraic model is established based on the projections of distorted receive waveforms onto the orthonormal basis given by the set of normalized orthogonal Hermite pulses. Using this new matrix model, a number of pulse-shape modulation schemes are analyzed and a novel orthogonal design is proposed. In the proposed orthogonal design, transmit waveforms are constructed as combinations of elementary Hermites with weighting coefficients derived by employing the Gram-Schmidt (QR) factorization of the differentiating distortion model's matrix. The design ensures orthogonality of the vectors at the output of the receiver bank of correlators, without requiring compensation for the distortion introduced by the antennas. In addition, a new set of elementary Hermite Pulses is proposed which further enhances the performance of the new design while enabling a simplified hardware implementation.**

Index Terms: **Pulse shape modulation, hermite pulses, orthogonal design, ultra-wideband.**

I. INTRODUCTION

Orthogonal pulses based on Hermite polynomials (Hermite pulses) for ultra-wideband (UWB) impulse radio (IR) communications has been proposed in [1]. Although other waveforms have recently been proposed for pulse-shape modulation (PSM) in UWB-IR systems (e.g., [2], [3]), Hermite pulses have a number of advantages over those waveforms.

First, Hermite pulses of different orders can easily be derived from successive transformations on the Gaussian pulse [4]. Second, these waveforms are well confined in both time and frequency, ensuring that all pulses have the same duration — which relates to achievable data-rate — while maximizing frequency efficiency. Third, although all Hermite pulses occupy the same bandwidth, their individual spectra are not identical, which implies that they can be used to combat frequency selectivity. Finally, Hermite pulses are orthogonal to one another, which suggests that a variety of designs making use of simultaneous pulse transmission can be considered.

For instance, in [5] Hermite pulses were combined so as to generate orthogonal waveforms with desired spectra. Pulse-Shape Modulation (PSM) based on Hermite pulses was proposed in [1] as an alternative to the conventional Pulse-Position Modulation (PPM) described in [6]. In [7] it is shown that the orthogonality of Hermite pulses can be further exploited to design combined pulse-shape and pulse position modulation (2-dimensional) schemes for UWB-IR systems in additive white Gaussian noise (AWGN) channels with significant data-rate improvement over their 1-dimensional counterparts. That work demonstrates that orthogonal pulse-shapes have the potential to enhance the performance of ultra-wideband systems beyond what is achievable with the conventional monocycles.

Although Hermite pulses are orthogonal when generated, cost effective and high-efficiency antennas are typically resistive-capacitive devices which often behave as differentiators [8], [9]. These devices modify both transmit and receive waveforms into scaled first and second-order derivatives of the originally generated orthogonal pulses. Consequently, elementary Hermite functions, such as those used in [5] and proposed in [1], result in received pulses which have polynomial (time-dependent) relationships to the generated pulses. In this case, unfortunately, the receive waveforms do not form an orthogonal set, implying that the results reported in [1] and [10] require integrators at the receiver. Given the extremely short duration of these waveforms (which prevents the possibility of numerical integration based on samples of the signal), their very low-power at the receiver (comparable to or lower than the noise-level) and the inevitable presence of noise and interference (which would be amplified and introduce instability and saturation problems), this requirement clearly poses a severe problem in implementation.

At the receiver, one alternative to the use of integrators is to generate template waveforms that are matched to receive pulses. This approach, however, is not only suboptimal - since these waveforms are not orthogonal - but also requires different transmit and receive waveform generators. Desirable performance will therefore not be achieved despite the additional hardware burden.

In other words, the design of PSM-UWB-IR communication systems and the application of Hermite pulses to such schemes are not as straightforward as suggested by [1].

In this paper, we reconsider the design of Hermite pulses for PSM in UWB-IR communications taking into account the distortive (differentiating) effect of antennas and focusing on performance while also considering the potential impact of the transceiver structure design on hardware implementation. A theoretical analysis of such distortion and its impact on the orthogonality of Hermite pulses is performed. Closed-form expressions for the cross-correlations between first derivatives (transmit), second derivatives (receive) and generated orthogonal Hermite pulses are given.

These equations yield the projections of the receive wave-

Manuscript received July 31, 2003.

The authors are with the Graduate School of Engineering, Division of Physics, Electrical and Computer Engineering, Yokohama National University, 79-5 Hodogaya, Yokohama, Japan 240-850, email: {giuseppe, craig,kohno}@kohnolab.dnj.ynu.ac.jp.

1229-2370/03/$10.00

forms onto the orthonormal basis formed by the elementary Hermite pulses. These projections are used to derive a new algebraic model of the distortive effects of transmit and receive antennas which are then represented by a single matrix. This matrix model of the distortive effect of antennas is used to derive a novel design method based on the Gram-Schmidt algorithm, which ensures orthogonality of the vectors at the output of the receiver bank of correlators without requiring integrators or different sets of pulse generators.

In order to enhance the performance of the proposed design while further reducing hardware requirements at the receiver, a new class of elementary Hermite pulses is also proposed. This new set of Hermite pulses has the property that the derivative of any pulse is also within the set. It is shown that under the assumption that antennas affect all pulses equally, the Gram-Schmidt-based orthogonal design yields better results when the proposed set of pulses is used.

The remainder of the paper is organized as follows. In Section II, a brief description of a basic pulse-shape modulation scheme for ultra-wideband communications is provided. In Section III, we analyze the properties of orthogonal Hermite pulses such as those proposed in [1] and their application to different types of pulse-shape modulation schemes. In Section IV, we introduce the proposed Gram-Schmidt-based design which yields orthogonal PSM schemes without the requirement of integrators at the receiver. The modified set of pulses that enhances the performance of the proposed orthogonalization procedure, while enabling implementation of the transceiver structure with reduced burden on hardware requirements, is then presented in Section V. Finally, conclusions are drawn in Section VI.

II. PULSE SHAPE MODULATION SCHEME

Let $n \in \{0, \cdots, N-1\}$ be the integer decimal equivalent to a binary codeword of length $\log_2(NL)$, where $N \in \mathbb{N}$ is a power of 2. Assume that N orthogonal waveforms $\lambda_n(t)$ of duration T seconds can be generated at the transmitter such that

$$\delta_{n,m} = \int_{-T/2}^{T/2} \lambda_n(t)\lambda_m(t)dt = \begin{cases} 0 & \text{if} \quad n \neq m \\ 1 & \text{if} \quad n = m \end{cases}, \qquad (1)$$

where without loss of generality we have considered all $\lambda_n(t)$ to have unitary energy.

If a source outputs a new codeword every T seconds, a simple N-ary pulse-shape modulation scheme maps each of these codewords onto a waveform $\lambda_n(t)$. Assuming a non-distortive channel, the received signal corresponding to the n-th codeword transmitted at time t_0 is given by

$$r(t - t_0 - \tau) = \alpha_n \lambda_n(t - t_0 - \tau) + w(t), \qquad (2)$$

where $w(t)$ is the additive noise (which may also model interference), τ is the time delay between transmitter and receiver and α_n is the path loss.

If perfect synchronization between transmitter and receiver is assumed, given the orthogonality property of the waveforms, the transmit codeword can be detected in a symbol-by-symbol maximum likelihood fashion by correlating the received signal with each of the N possible waveforms.

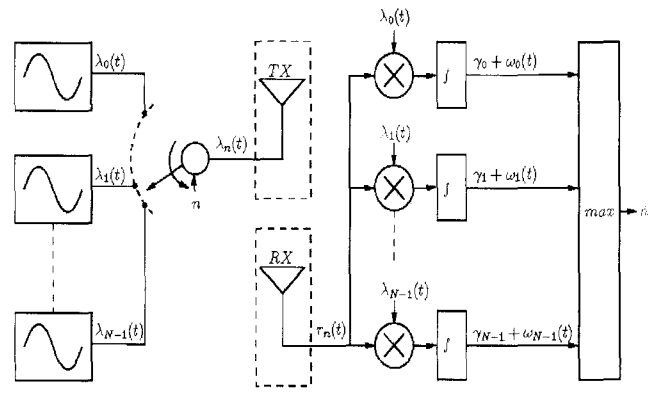

Fig. 1. Structure of a simple PSM-UWB-IR system. The transmitter transmits one of N orthogonal waveforms. The receiver makes a maximum likelihood decision based on the comparison of the received signal with N template waveforms.

Let each correlator output a test statistic γ_n defined as,

$$\gamma_n = \int_{-T/2}^{T/2} r(t - t_0 - \tau)\lambda_n(t - t_R)dt. \qquad (3)$$

With perfect synchronization, $t_R = t_0 + \tau = 0$ and the detection process can be described mathematically by

$$\hat{n} = \frac{1}{N}\left\{n \;\middle|\; \gamma_n > \gamma_m \; \forall \, m\right\}. \qquad (4)$$

The binary codeword corresponding to the estimate $\hat{n}$ is therefore the symbol-by-symbol maximum likelihood estimate of the transmit symbols.

A schematic diagram of the PSM-UWB-IR system is shown in Fig. 1.

The performance of such a system is clearly dependent on the auto- and cross-correlation properties of the waveforms used to represent the symbols n associated with the binary transmit codewords.

Assume that the noise $w(t)$ disturbing the received signal is AWGN with zero mean and variance σ_w^2. If the receive correlators are noiseless and have normalized energy, the noise processes observed at the output of each of the correlators are independent and identically distributed (i.i.d.), with zero mean and variance σ_w^2/N [11]. Therefore, the probability density function of the random process w_n is given by

$$P_{\mathrm{w}}\left(w_n; 0, \frac{\sigma_w^2}{N}\right) = \frac{1}{\sigma_w}\sqrt{\frac{N}{2\pi}}e^{-\frac{N w_n^2}{2\sigma_w^2}}. \qquad (5)$$

The probability $P_{n\to m}$ that an erroneous decision in favor of the m-th symbol is made when the n-th order symbol is transmitted is given by the probability that the output of the m-th correlator (w_m) is larger than the output of the n-th correlator $(\alpha_n + w_n)$.

Given the independency of the random processes w_n and w_m,

we have

$$P_{n\to m} = \int_{-\infty}^{\infty} P_{\mathrm{w}}\left(w_n; 0, \frac{\sigma_w^2}{N}\right) \cdot \int_{\alpha_n + w_n}^{\infty} P_{\mathrm{w}}\left(w_m; 0, \frac{\sigma_w^2}{N}\right) dw_m dw_n$$

$$= \sqrt{\frac{N}{8\pi\sigma_w^2}} \int_{-\infty}^{\infty} \mathrm{erfc}\left(\sqrt{\frac{N}{2}} \frac{\alpha_n + w_n}{\sigma_w}\right) e^{-\frac{N w_n^2}{2\sigma_w^2}} dw_n, \quad (6)$$

where $\mathrm{erfc}(\cdot)$ is the complementary error function [11].

Now, the probability that the n-th waveform is erroneously detected as any other waveform is simply

$$P_E(n) = \sum_{\substack{m=0 \\ m\neq n}}^{N-1} P_{n\to m}. \quad (7)$$

Finally, if P_n denotes the probability with which the source outputs the n-th codeword, the symbol error probability P_{E_S} is given by

$$P_{E_S} = \sum_{n=0}^{N-1} P_n P_E(n). \quad (8)$$

In most practical cases, all symbols in the transmit alphabet have equal likelihood such that the averaged bit error probability P_{E_B} is related to the symbol error probability by [11],

$$P_{E_B} = \frac{N}{2(N-1)} P_{E_S}. \quad (9)$$

A more detailed analysis of the performance of this pulse-shape modulation scheme for ultra-wideband communications and the derivation of closed-form expressions for the probabilities given above are beyond the scope of this paper. The basic description and analysis of the pulse-shape modulation presented are enough to understand that the performance of such a scheme deteriorates if one or more of the following can be said:

1. *The waveforms $\lambda_n(t)$ are not orthogonal at the receiver.*
2. *The received waveforms are not matched to the templates available at the receiver.*
3. *For arbitrary $\lambda_n(t)$ and $\lambda_m(t)$, $\alpha_n > \alpha_m$ while $P_n < P_m$.*

Item 1 implies that the distances between the outputs of the correlators are not maximized and often not equal. This increases the probability of mistaking one pulse for another in the presence of noise, typically introducing biased errors to the system.

Item 2 implies that the distance between the signal and noise subspaces is shorter, which reduces the ability of the system to distinguish received signals from noise. This typically increases the probability of error uniformly over all symbols. A possible cause for items 1 and 2 is pulse distortion.

Finally, item 3 is related to well-known information-theoretical results on efficient encoding. Symbols with higher likelihood should be mapped onto waveforms with better auto- and cross-correlation properties. Typically, however, the equal likelihood of all symbols requires all waveforms to have similar properties in order to maximize performance [12].

In the next section, we analyze the properties of orthogonal Hermite pulses, which have been proposed for pulse-shape modulated ultra-wideband systems [1].

III. ANALYSIS OF CONVENTIONAL HERMITE PULSES

A. Orthogonality of Hermite Pulses

Let the n-th order Hermite polynomial be defined in the interval $-\infty < t < \infty$ of a normalized time scale by the Rodrigues formula as follows [13]

$$H_n(t) \equiv (-1)^n e^{t^2} \frac{d^n}{dt^n} e^{-t^2} \quad n \in \mathbb{N}. \quad (10)$$

The following useful relations among these Hermite polynomials are known [13], [14]:

$$H_{n+1}'(t) = 2(n+1)H_n(t) \quad (11a)$$

$$H_{n+2}(t) = 2tH_{n+1}(t) - 2(n+1)H_n(t) \quad (11b)$$

$$nH_{n+1}(t) = tH_{n+1}'(t) - (n+1)H_n'(t) \quad (11c)$$

$$\int_{-\infty}^{\infty} e^{-t^2} H_n(t)H_m(t)dt = \begin{cases} 0 & \text{if } n \neq m \\ 2^n n!\sqrt{\pi} & \text{if } n = m, \end{cases} \quad (11d)$$

where $H'(t)$ denotes the first derivative of $H(t)$ with respect to t.

Waveforms with finite duration (pulses) can be constructed based on Hermite polynomials by multiplying them with an exponentially decaying coefficient as follows

$$\psi_n(t) \equiv \mathcal{N}_n e^{\frac{-t^2}{a}} H_n(t) \quad a > 0, \quad (12)$$

where $\mathcal{N}_n$ is a factor that normalizes the energy of $\psi_n(t)$ and a is a positive constant.

In this paper, the waveforms given in (12) are referred to as Hermite pulses or simply *Hermites*.

Using properties (11a) through (11c), it is easy to find that the first and second derivatives of (12) are given by equations (13a) and (13b), respectively.

$$\psi_n'(t) = \mathcal{N}_n e^{\frac{-t^2}{a}} \left[2\left(\frac{a-1}{a}\right)^2 H_n(t) - H_{n+1}(t)\right] \quad (13a)$$

$$\psi_n''(t) = \mathcal{N}_n e^{\frac{-t^2}{a}} \times \left[\left[4t^2\left(\tfrac{a-1}{a}\right)^2 - 2\left(\tfrac{an+1}{a}\right)\right]H_n(t) - 2t\left(\tfrac{a-2}{a}\right)H_{n+1}(t)\right]. \quad (13b)$$

In the special case when $a = 2$, (11d) can be used not only to determine the normalization coefficient $\mathcal{N}_n$ for the waveform given in (12), but also to establish the orthogonality of the waveforms given by

$$\psi_n(t) = \frac{e^{\frac{-t^2}{2}} H_n(t)}{\sqrt{2^n n!\sqrt{\pi}}}. \quad (14)$$

These are in fact the pulses used in [5] and are hereafter referred to as *orthogonal* Hermite pulses. An alternative definition of orthogonal Hermite pulses was used in [1], but it has

been shown in [15] that both waveforms are equivalent, differing only in the normalized time scale used. The results of the analysis that follows therefore holds for both of these definitions of orthogonal Hermite pulses.

Substituting $a = 2$ into (13a) and (13b), we obtain:

$$\psi_n^{'}(t) = t\psi_n(t) - \frac{\mathcal{N}_n}{\mathcal{N}_{n+1}}\psi_{n+1}(t), \tag{15a}$$

$$\psi_n^{''}(t) = (t^2 - 2n - 1)\psi_n(t). \tag{15b}$$

The cross-correlations of the first derivatives of orthogonal Hermites given in (15a) contain terms on $t^2H_n(t)H_m(t)$, $tH_n(t)H_m(t)$ and $H_n(t)H_m(t)$, which do not vanish for all pairs of n and $m \in \mathbb{N}$. These cross-correlations are given by

$$R_{\psi'}(n,m) = \int_{-\infty}^{\infty} \psi_n^{'}(t)\psi_m^{'}(t)dt \tag{16}$$

$$= \frac{D(n+1,m+1) - E(n+1,m) - E(n,m+1) + F(n,m)}{\sqrt{2^{n+m}n!m!\pi}},$$

where the functions $D(n,m)$, $E(n,m)$ and $F(n,m)$ are given in the appendix.

Analogously, the cross-correlations of the second derivatives of these waveforms, given in (15b), are

$$R_{\psi''}(n,m) = \int_{-\infty}^{\infty} \psi_n^{''}(t)\psi_m^{''}(t)dt = \tag{17}$$

$$\frac{(4nm+2n+2m+1)D(n,m) - 2(n+m+1)F(n,m) + G(n,m)}{\sqrt{2^{n+m}n!m!\pi}},$$

where the function $G(n,m)$ is also given in Appendix.

It is clear from (16) and (17) that the first or second derivatives of orthogonal Hermites no longer form orthogonal sets. Since many of the efficient and cost effective antennas that can be manufactured in small sizes are resistive-capacitive devices with differentiating behaviors [8], [9], such differentiation distortion cannot be neglected if Hermite polynomial-based waveforms are to be considered for UWB impulse radio communications. In the next subsection, the performance of orthogonal Hermites in the presence of such differentiating antennas is characterized in further detail.

B. Efficient Differentiating Antennas

Consider a resistive-capacitive differentiating antenna with the following response to an input waveform $f(t)$ [9]

$$\mathcal{F}(t) = \eta f^{'}(t), \tag{18}$$

where η is an efficiency coefficient.

It is assumed that the antenna has reciprocal performances at transmission and reception, and that its efficiency is the same for all pulses considered. Without loss of generality, the antenna efficiency is normalized to the unit, which means that the energy of the waveform output by the antenna is 1.

Mathematically, the normalized efficiency condition can be stated as follows. Let the input to the antenna be one of the waveforms $f_n(t)$ where $n \in 0, \cdots, N-1$. Then we have,

$$\eta_n^2 \int_{-\infty}^{\infty} \left(f_n^{'}(t)\right)^2 dt = 1 \ \forall\, n. \tag{19}$$

Given the orthogonal Hermite pulses defined in (14) and the cross-correlation values in (16), the efficiency coefficient of the transmit antenna is given by

$$\eta_{\text{TX}}(n) = \frac{1}{\sqrt{R_{\psi'}(n,n)}} = \frac{1}{\sqrt{\left(n+\frac{1}{2}\right)}}. \tag{20}$$

Consequently, the unitary-energy transmit waveform corresponding to the n-th orthogonal pulse is

$$\varphi_n(t) = \eta_{\text{TX}}(n)\psi_n^{'}(t). \tag{21}$$

These transmit waveforms may undergo further distortion and disturbances in the channel caused by various effects such as frequency selectivity, shadowing, jitter etc. In this paper, however, such channel effects are set aside for the following reasons.

First, this contributes to a better theoretical knowledge and insight on the impact of the differentiating distortion on the properties of orthogonal Hermite pulses for UWB-IR communications.

Second, theoretical [6], [16], [17] and practical evidence are available to support the fact that impulse-based architectures of UWB impulse radios have the potential to operate on signals (impulse) that achieve extremely high "time-of-arrival resolution", enabling RAKE-like receivers to mitigate multipath and translate the channel essentially into a distortion-plus-noise channel.

Third, the theory presented can be (and has been, to a certain extent [18], [19]) extended to application in a variety of distortive effects, either in isolation or in combination. In [18] and [19], for instance, the effect of jitter in isolation and in combination with differentiating distortion were respectively considered.

Fourth, although numerous works on channel models and measurement for UWB signals have been published, (e.g., [20], [21], and [22]), the results still appear to be preliminary. This is largely because the frequency responses of transmit/receive antennas used in experiments are not the same as those that are likely to be used in real systems. In addition, equipment used in channel sounding has limited bandwidth (typically not much more than 1 GHz) compared to those considered for commercial UWB systems (several GHz).

In fact, such UWB channel models (which indicate severe multipath conditions) are in general SISO models which do not include the potential of space-time equalization or beamforming. In [23], however, it has been shown that wavelet designs can be effectively used to obtain beamforming arrays for UWB transmission. Further development in this area may have impact on channel models for UWB-IR communications.

Fifth, the very idea of utilizing orthogonal waveforms in the design of UWB impulse radios offers the possibility of alternative architectures (previously not thought of) which, in similarity to OFDM systems, have the potential to transform an interfering multipath channel into a distortive channel. In this case, the theory presented here can once again be extended and utilized to combat such distortion.

All the above suggests that at this point in time it is prudent not to assume any particular distortive propagation channel

model. Again, it must be emphasized that the method that will be introduced in this paper can be easily extended to incorporate any channel models, as long as their mathematical descriptions are known.

For these reasons, in this paper, the only additional distortion considered to affect transmit waveforms given in (21) is a second differentiation introduced by the receive antenna.

If the transmit waveforms are received by an efficient differentiating antenna, the receive waveform corresponding to the n-th order Hermite pulse generated at the transmitter is

$$\phi_n(t) = \eta_{\text{RX}}(n)\eta_{\text{TX}}(n)\psi_n''(t). \tag{22}$$

From (17) and (22), the efficiency coefficient of the receive antenna is

$$\eta_{\text{RX}}(n) = \frac{1}{\eta_{\text{TX}}(n)\sqrt{\frac{3}{2}\left(n^2+n+\frac{1}{2}\right)}}. \tag{23}$$

Equation (22) signifies that the receive waveforms corresponding to orthogonal Hermites generated at the transmitter are simply normalized second derivatives of the generated pulses.

On the other hand, it was shown above that the second derivatives of Hermites are not orthogonal. This analysis suggests that in order to achieve the results reported in [1] and [5], a pair of integrators is required at the receiver. Given the short duration of UWB pulses and their low power (comparable to noise), it is clear that this alternative in not practical.

If receive signals cannot be integrated at the receiver, detection can be carried out by comparison with a set of locally generated waveforms. In the next section we consider two alternatives of such detectors, namely a *matched* and a *non-matched* receiver. In the matched receiver, received waveforms are compared to the normalized second derivatives of the orthogonal Hermite pulses, while in the non-matched receiver, these waveforms are compared to the same set of pulses used at transmission.

C. PSM Scheme with Matched Receiver

Consider a PSM-UWB-IR system with an alphabet of N Hermite pulses $\psi_n(t)$ with orders ranging from 0 to $N-1$. The output of the m-th correlator is given by

$$R_\phi(n,m) = \int_{-\infty}^{\infty} \phi_n(t)\phi_m(t)dt = \tag{24}$$
$$\frac{(4nm+2n+2m+1)D(n,m)-2(n+m+1)F(n,m)+G(n,m)}{\frac{3}{2}\sqrt{\left(n^2+n+\frac{1}{2}\right)\left(m^2+m+\frac{1}{2}\right)2^{n+m}n!m!\pi}}.$$

Table 1 gives a few numeric values obtained with (24). The results in Table 1 suggest that two different detection schemes can be considered for the matched receiver. In a non-coherent scheme, where the receiver does not know whether the pulses arrive inverted or not, only the magnitudes of $R_\phi(n,m)$ are taken into account. The n-th pulse is detected if the absolute value of the output of the n-th correlator is largest. Mathematically, we have

Table 1. Correlator outputs for matched receiver.

$a=2$		Order of $\phi_m(t)$							
		0	1	2	3	4	5	6	7
Order of $\phi_n(t)$	0	1	0	−0.784	0	0.255	0	0	0
	1	0	1	0	−0.730	0	0.209	0	0
	2	−0.784	0	1	0	−0.700	0	0.190	0
	3	0	−0.730	0	1	0	−0.687	0	0.182
	4	0.255	0	−0.700	0	1	0	−0.680	0
	5	0	0.209	0	−0.687	0	1	0	−0.677
	6	0	0	0.190	0	−0.680	0	1	0
	7	0	0	0	0.182	0	−0.677	0	1

$$\hat{n} = \left\{k \;\middle|\; |R_\phi(n,k)| > |R_\phi(n,m)| \;\forall\, m\right\}. \tag{25}$$

Table 1 clearly shows that only waveforms corresponding to even and odd order transmit pulses are orthogonal. Consequently, the output vectors corresponding to transmit waveforms of orders m and n are highly correlated if $|m-n|$ is a multiple of 2 ($|\cdot|$ denotes the absolute value). In other words, receive vectors corresponding to even (odd) transmit pulses are not mutually orthogonal and may in fact be separated by significantly small angles.

In a coherent scheme, where the receiver knows whether pulses are inverted or not, the whole vector output by the bank of correlators can be compared to those given by

$$\mathbf{r}_n = [R_\phi(n,0) \quad \cdots \quad R_\phi(n,N-1)]^{\text{T}}. \tag{26}$$

Let $\tilde{\mathbf{r}}_n = \mathbf{r}_n + \mathbf{w}$ be the received vector corresponding to a transmit pulse of order n, where $\mathbf{w}$ is a noise vector. The n-th pulse is detected if the projection of $\tilde{\mathbf{r}}_n$ onto $\mathbf{r}_n$ is larger the the projections of $\tilde{\mathbf{r}}_n$ onto all remaining $\mathbf{r}_m$. Mathematically, we have

$$\hat{n} = \left\{k \;\middle|\; \frac{\mathbf{r}_k}{|\mathbf{r}_k|}\cdot\tilde{\mathbf{r}}_n > \frac{\mathbf{r}_m}{|\mathbf{r}_m|}\cdot\tilde{\mathbf{r}}_n \;\forall\, m\right\}. \tag{27}$$

It is clear that the (vector-wise comparison) coherent scheme will perform significantly better than a (pairwise comparison) non-coherent one since their maximum likelihood properties are better. This implies that orthogonal designs that are based on the vectors given by the correlator outputs have higher potential to reach capacity than schemes such as those proposed in [1].

With coherent detection, it is desirable that the vectors given in (26) representing the output of the bank of correlators (rows of Table 1) are orthogonal and have lengths that are as large as, and as uniform as possible. A hypothetical optimal example would be a system that yields orthogonal vectors whose entries are either $+1$ or -1, such as Walsh codes. Unfortunately, such a scheme is impossible since no signal can be fully correlated to more than one distinct template.

While the coherent detection using conventional Hermites yields an improvement over a non-coherent strategy (at the cost

Table 2. Correlator outputs for non-matched receiver.

$a=2$		Order of $\psi_m(t)$							
		0	1	2	3	4	5	6	7
Order of $\varphi_m(t)$	0	−0.577	0	0.817	0	0	0	0	0
	1	0	−0.775	0	0.633	0	0	0	0
	2	0.227	0	−0.801	0	0.555	0	0	0
	3	0	0.283	0	−0.808	0	0.516	0	0
	4	0	0	0.312	0	−0.812	0	0.494	0
	5	0	0	0	0.330	0	−0.813	0	0.479
	6	0	0	0	0	0.343	0	−0.814	0
	7	0	0	0	0	0	0.352	0	−0.815

of an additional complexity introduced by the need for channel estimation), it is clear that the output vectors are still not orthogonal. In other words, the performance of this matched receiver, be it coherent or non-coherent, is still sub-optimal because the set of elementary pulses used (conventional Hermites) is designed to be orthogonal.

One disadvantage of the matched scheme, however, is the need for using distinct sets of waveform generators at transmission and reception. An alternative non-matched receiver which avoids this additional burden on hardware requirements is analyzed in the next subsection.

D. PSM Scheme with Non-Matched Receiver

Consider a PSM system whose transmit waveforms are defined by (21), as in Section III-C, but that utilizes the same bank of waveform generators for transmission and reception. As before, the waveform corresponding to a transmit n-th order pulse will be given by (22), so that the m-th correlator output is

$$R_{\phi\psi}(n,m) = \int_{-\infty}^{\infty} \phi_n(t)\psi_m(t)dt \qquad (28)$$
$$= = \frac{F(n,m) - (2n+1)\,D(n,m)}{\sqrt{\frac{3}{2}\left(n^2+n+\frac{1}{2}\right)2^{n+m}n!m!\pi}}.$$

Table 2 gives a few numerical values obtained with (28) for an 8-ary PSM system. It is clear that a coherent detection scheme can be constructed for the non-matched receiver just as done in the previous subsection for the matched receiver.

The equivalent of (25) becomes

$$\hat{n} = \left\{k \;\middle|\; |R_{\phi\psi}(n,k)| > |R_{\phi\psi}(n,m)|\ \forall\, m\right\}. \qquad (29)$$

From Table 2, it is seen that the absolute values of the diagonal entries are larger than those of the off-diagonal entries, except for the 0-th order pulse. If the 0-th order pulse is excluded from the alphabet, a non-coherent scheme similar to that described in the previous subsection can also be considered.

In either case it is evident that the non-matched receiver incurs a higher loss of energy than the matched receiver since the length of the received vectors are lower than those in the latter case. Nonetheless, the non-matched scheme does not require different sets of waveform generators at transmission and reception and is therefore simpler to implement.

In the next subsection, simulation results on the performances of the two PSM schemes discussed so far are given.

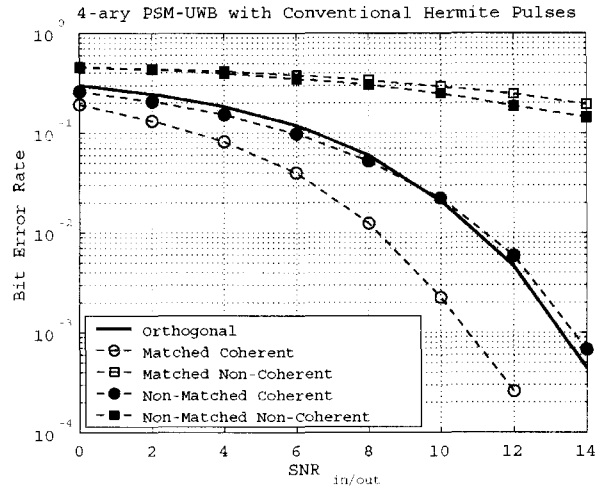

Fig. 2. Bit error rate performances of 4-ary pulse-shape modulated ultra-wideband systems. Curves for orthogonal, matched and non-matched schemes with coherent and non-coherent detection are shown.

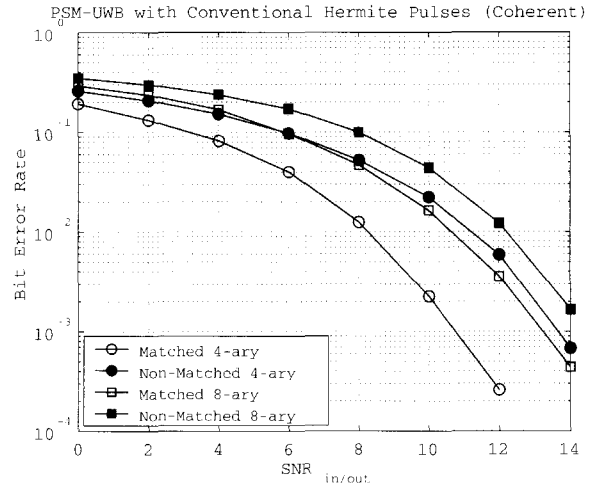

Fig. 3. Bit error rate performances of 4-ary and 8-ary pulse-shape modulated ultra-wideband systems. Only curves for coherent detection schemes are shown.

E. Performance of PSM Schemes with Hermite Pulses

Figs. 2 and 3 compare the bit error rate performances of pulse-shape modulation schemes using Hermite pulses.

The signal-to-noise ratio ($\mathrm{SNR}_{\mathrm{in/out}}$) against which error rates are plotted is defined as the ratio between the signal power at the receive antenna (which is normalized to the unit) and the total noise at the output of the bank of correlators. The reason that such an input-power-to-output-noise ratio figure (thus the sub-index $_{\mathrm{in/out}}$) is used, is that the correlations performed with matched and non-matched filters result in different amounts of energy transferred to the output in each scheme. Defined in this way, $\mathrm{SNR}_{\mathrm{in/out}}$ takes into account the inefficiency of non-

matched correlators, allowing for a fair comparison between the two alternatives.

It is clear that two complementary ways to enhance the performance of a PSM scheme are to increase the efficiency of the bank of correlators (matched/non-matched), and to increase the portion of energy effectively used in the detection process (coherent/non-coherent). The above signal to noise ratio measure enables us to quantify the total gain in performance resulting from both strategies, as done in Sections IV and V.

In Fig. 2, matched and non-matched 4-ary PSM schemes with coherent detection are compared to those with non-coherent detection. The performance of a PSM scheme with orthogonal pulses (equivalent to the assumption that antennas are not differentiating devices) as that proposed in [1] is also shown. Note that in this ideal case when the set of received pulses are mutually orthogonal, coherent and non-coherent detections are equivalent, which implies that the performance of the PSM scheme with orthogonal pulses can be interpreted as the lower bound to the performance of non-coherent methods. It is shown, however, that a vector-based PSM scheme with a non-matched receiver and coherent detection performs nearly as well as the orthogonal pulse-based PSM system despite the differentiating effect of the antennas. Moreover, it is also observed that the vector-based PSM scheme with matched receiver and coherent detection outperforms orthogonal pulse-based PSM, even in the presence of differentiating antennas.

These results are due to two major factors. The first is that with a set of pulses which are non-orthogonal at the receiver, a larger amount of energy is retained through the correlation process, as discussed in the previous subsection. In other words, a larger number of correlator outputs are non-zero in the presence of a received pulse and a larger proportion of the received energy is effectively utilized in the detection process. The second, and perhaps more important factor, is that a vector-based scheme enhances the maximum-likelihood properties of the correlation-based receiver because, among other reasons, the influences of noise, distortion and other effects are averaged across the entries of the vectors (assuming that these are independent at different correlators).

In general, Fig. 2 demonstrates that the matched receiver outperforms the non-matched one, and that coherent detection outperforms non-coherent detection. The fact that matched receivers significantly outperform non-matched ones is further emphasized by Fig. 3, which compares 4-ary and 8-ary PSM schemes with coherent detection.

Another important conclusion that can be drawn from the results shown in Fig. 3 is that in a vector-based (coherent) pulse-shape modulation scheme, the performance of the system can degrade significantly with the order of the modulation. For instance, it is seen in the plot that 8-ary PSM performs worse than 4-ary, both with matched and non-matched receivers.

This is because, as can be seen from Table 1 and Table 2, the length of the vector output by the bank of correlators in the presence of an n-th order receive pulse (n-th rows in the tables) reduces with n.

In summary, if non-coherent detection (as defined in this paper) is employed, a set of pulses that exhibit orthogonality at the receiver would yield optimal results (see bold curve in Fig. 2). To date, however, no systematic method to design waveforms that exhibit orthogonality at the receiver in the presence of distortion, such as differentiating antennas, is known. Among the known pulse shapes proposed for non-coherent PSM schemes, such as [2], [3], [5], Hermite pulses seem to be best due to their good time-frequency confinement and systematic design. It was however shown here that in the presence of commonly used differentiating antennas, Hermite pulses are no longer orthogonal at the receiver unless a double integration is performed. To the best of our knowledge, works on PSM-UWB-IR systems have focused on such a non-coherent detection approach, while the results shown here clearly indicate that this scheme is suboptimal compared to a vector-based (coherent) PSM system.

Coherent schemes only require the additional knowledge of whether pulses are inverted or not. This is easily achieved using the pilot symbols already available from synchronization and is clearly simpler than double-integration. We therefore maintain that a better approach is to design PSM systems with vector-based coherent detection. Note, however, that while Fig. 2 supports this idea, Fig. 3 shows that if the receive vectors are *not orthogonal*, the performance enhancement achieved with the introduction of a matched bank of correlators may be inconsistent when observed in PSM of different orders. For instance, Fig. 3 shows that a matched 4-ary PSM scheme outperforms a non-matched by a larger margin than observed with the corresponding 8-ary schemes. The reason is that while the matched receive vectors always have larger norms than non-matched receive vectors, the effect of matched/non-matched correlators on the distance (angles) between different possible vectors is unclear in a non-orthogonal scheme. Since detection ultimately depends on both of these properties, this accounts for an inconsistent behavior of *non-orthogonal* vector-based PSM schemes.

In other words, while coherent detection is superior to non-coherent PSM, orthogonality among the received vectors is also required for optimal performance. In the next section, a new design of transmit waveforms and receive templates is proposed in order to achieve this. Further, in Section V, we introduce a new set of elementary Hermite pulses that not only improves the proposed orthogonal vector-based PSM design, but also enables the use of the same set of generators for transmission and reception. The combination of these two proposed techniques enables the design of high-performance orthogonal PSM systems with simple hardware implementation.

IV. ORTHOGONAL DESIGN OF HERMITE PULSES

A. Differentiating Distortion Model

Assuming that the transceivers can only generate the same set of elementary Hermite pulses $\psi_n(t)$, the noiseless UWB link established between the transmitter's bank of pulse generators and the receiver's bank of correlators can then be modelled as a N-by-N matrix defined by

$$\mathbf{C} = \begin{bmatrix} c_{0,0} & c_{0,1} & \cdots & c_{0,N-1} \\ c_{1,0} & c_{1,1} & \cdots & c_{1,N-1} \\ \vdots & \vdots & \ddots & \vdots \\ c_{N-1,0} & c_{N-1,1} & \cdots & c_{N-1,N-1} \end{bmatrix} \tag{30}$$

where, for the case of a matched bank of correlators, the entries $c_{n,m}$ are given by (see (24))

$$c_{n,m} = R_{\phi}(n,m). \tag{31}$$

Analogously, for the case of a non-matched bank of correlators, $c_{n,m}$ are obtained from (28), giving

$$c_{n,m} = R_{\phi\psi}(n,m). \tag{32}$$

Let the n-th order transmit pulse be represented by a vector

$$\mathbf{t}_n = \left[\begin{array}{ccc} \delta_{n,0} & \cdots & \delta_{n,N-1} \end{array} \right]^{\mathrm{T}}, \tag{33}$$

where $\delta_{n,m}$ is the Kronecker delta and $[\cdot]^{\mathrm{T}}$ denotes the transpose operation.

Then, at the receiver, the vector output by the bank of correlators can be written as

$$\mathbf{r}_n = \mathbf{C} \cdot \mathbf{t}_n = \left[\begin{array}{ccc} c_{0,n} & \cdots & c_{N-1,n} \end{array} \right]^{\mathrm{T}}. \tag{34}$$

Note that the simple model presented here significantly reduces the complexity involved in dealing with the distortive effect that antennas introduce in UWB-IR communications. In fact, taking the projections of the distorted (second-derivative) waveforms onto the space of the receiver's bank of correlators, we transform a convolutional distortion (second order derivative) into a simple multiplicative model. This enables the use of simple, yet effective, mathematical tools to process the transmit and received pulses in order to ensure the orthogonality of received vectors.

B. Design Method

The fact that orthogonal Hermite pulses are no longer orthogonal at the receiver is reflected by the distortion matrix $\mathbf{C}$ not being diagonal, which implies that $\mathbf{r}_n \cdot \mathbf{r}_m \neq 0$ for all $n \neq m$.

It is however easy to verify that $\mathbf{C}$ has full-rank. Consequently, there is an orthogonal matrix $\mathbf{Q}$ and an upper-triangular matrix $\mathbf{R}$ such that [24]

$$\mathbf{C} = \mathbf{Q} \cdot \mathbf{R}. \tag{35}$$

Let $\mathbf{X}$ be the inverse of $\mathbf{R}$, such that

$$\mathbf{Q} = \mathbf{C} \cdot \mathbf{X}. \tag{36}$$

Then, if the n-th column of $\mathbf{X}$ is used to represent the n-th symbol in the transmit alphabet, the corresponding receive vector is the n-th column of $\mathbf{Q}$, which is orthogonal.

Let the m-th order proposed pulse be constructed by the combination of elementary Hermite pulses, using the entries of the m-th column of $\mathbf{X}$ as coefficients. The m-th generated orthogonalized pulse is

$$\xi_m(t) = \mathcal{M}_m \sum_{n=0}^{N-1} x_{n,m} \psi_n(t), \tag{37}$$

where $x_{n,m}$ denotes the n-th element in the m-th column of $\mathbf{X}$ and $\mathcal{M}_m$ is a normalization factor.

If it is assumed that the transmit antenna is efficient, as defined in Section III-B, the transmit waveform corresponding to a generated elementary Hermite pulse of order n is $\varphi_n(t)$, given by (21). Consequently, the transmit waveform corresponding to a generated $\xi_m(t)$ is simply

$$\zeta_m(t) = \mathcal{M}_m \sum_{n=0}^{N-1} x_{n,m} \eta_{\mathrm{TX}}(n) \psi_n'(t) = \mathcal{M}_m \sum_{n=0}^{N-1} x_{n,m} \varphi_n(t). \tag{38}$$

The normalization factor $\mathcal{M}_m$ can then be calculated from

$$\int_{-\infty}^{\infty} \zeta_m(t)^2 dt = \mathcal{M}_m^2 \int_{-\infty}^{\infty} \left(\sum_{n=0}^{N-1} x_{n,m}(t) \varphi_n(t) \right)^2 dt = 1, \tag{39}$$

where we have used the fact that the waveforms $\varphi_n(t)$ are normalized.

Using (16) we obtain

$$\mathcal{M}_m = \left(\sqrt{ \sum_{n=0}^{N-1} x_{n,m}^2 + \sum_{\substack{n,p=0 \\ n \neq p}}^{N-1} \frac{x_{n,m} x_{p,m} \left(R_{\psi'}(n,p) + R_{\psi'}(p,n) \right)}{\sqrt{\left| R_{\psi'}(n,n) + R_{\psi'}(p,p) \right|}} } \right)^{-1}. \tag{40}$$

The method described above means that instead of mapping a binary codeword onto a single orthogonal Hermite pulse, we

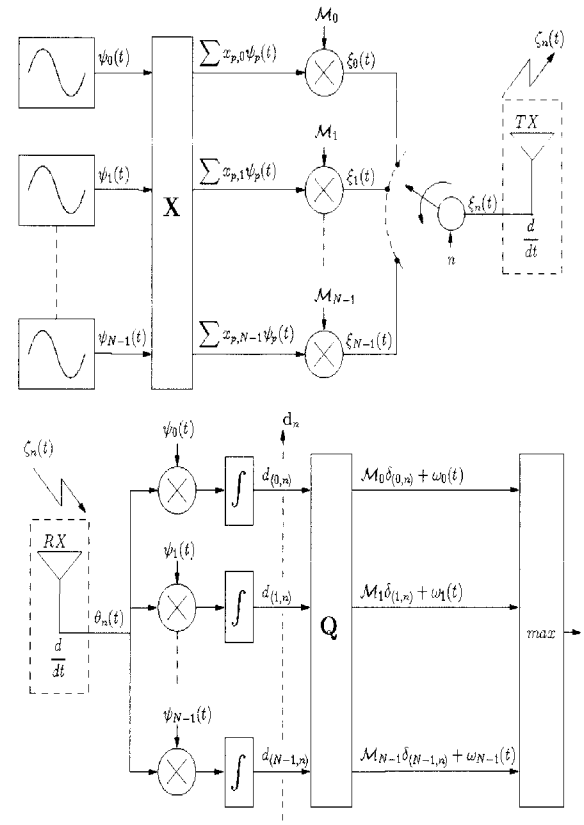

Fig. 4. Proposed PSM scheme employing a non-matched bank of correlators. The equivalent for the case of a matched bank of correlators is obtained by replacing $\psi_n(t)$ with $\phi_n(t)$.

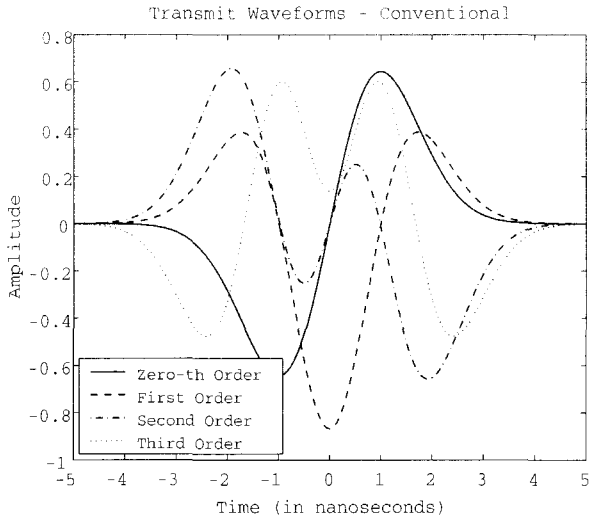

Fig. 5. Transmit waveforms obtained with proposed orthogonal design using conventional Hermite pulses as elementary components

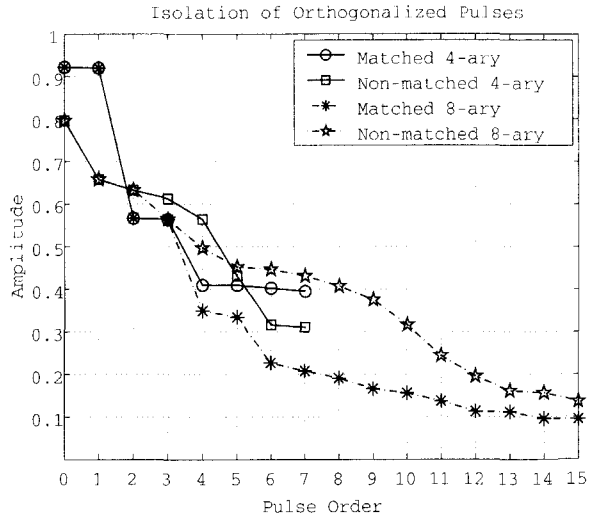

Fig. 6. Amplitude of the isolation coefficients ($\mathcal{M}_n$) of orthogonalized Hermite pulses with matched and non-matched banks of correlators at receiver.

map each binary codeword onto a symbol constructed as a combination of orthogonal Hermite pulses, as illustrated in Fig. 4.

It is known from [4] that the complexity involved in generating an n-th order Hermite pulse increases with n. In addition, the higher the order of an elementary orthogonal Hermite pulse, the larger the number of zero-crossings observed in its waveforms, i.e., the higher the precision required to generate it and thus the more prone it is to distortion.

This means that higher order pulses should have as little relevance as possible in the lower order combined waveforms. This is the reason that the Gram-Schmidt algorithm (QR-factorization) is preferred, as opposed to other orthogonalization methods such as the eigen or singular value decompositions.

Indeed, since $\mathbf{R}$ is upper-triangular, so is its inverse $\mathbf{X}$. The last $N-m-1$ elements of the m-th column of $\mathbf{X}$ are therefore all zero, which means that an m-th order pulse requires the combination of only the first (lower order) $m+1$ orthogonal Hermite pulses in order to be generated. Consequently, the pulses obtained have a desirable lower reliance on higher order waveforms than if the above-mentioned orthogonalization techniques were used.

Fig. 5 shows a few of the waveforms obtained with the proposed design using a set of four orthogonal Hermite pulses as elementary components.

At the output of an efficient differentiating receive antenna, the waveform corresponding to a transmit pulse $\zeta_m(t)$ is given by

$$\theta_n(t) = \mathcal{M}_m \sum_{n=0}^{N-1} x_{n,m}\eta_{\mathrm{RX}}(n)\varphi_n'(t) = \mathcal{M}_m \sum_{n=0}^{N-1} x_{n,m}\phi_n(t). \tag{41}$$

At the output of the bank of correlators, the following receive vector is obtained:

$$\mathbf{d}_n = \begin{bmatrix} d_{n,0} & \cdots & d_{n,N-1} \end{bmatrix}^{\mathrm{T}}, \tag{42}$$

where noise has been omitted.

These vectors, in turn, are orthogonal to the template receive vectors given by the columns of $\mathbf{Q}$. Thus, we have

$$\mathbf{d}_n \cdot \mathbf{q}_m = \begin{cases} 0 & \text{if } n \neq m \\ \mathcal{M}_n & \text{if } n = m \end{cases}. \tag{43}$$

Making use of the Kronecker delta, the output of the m-th correlator to an input n-th order pulse can be simply rewritten as $\mathbf{d}_n \cdot \mathbf{q}_m = \mathcal{M}_n \delta_{n,m}$.

Denoting the noisy receive vector by $\tilde{\mathbf{d}}_n = \mathbf{d}_n + \mathbf{w}$, detection is then carried out by comparison with the columns of $\mathbf{Q}$. Mathematically we have

$$\hat{n} = \left\{ k \;\middle|\; \mathbf{q}_k \cdot \tilde{\mathbf{d}}_n > \mathbf{q}_m \cdot \tilde{\mathbf{d}}_n \;\forall\, m \right\}. \tag{44}$$

C. Properties of the Proposed Design

Although all columns of $\mathbf{Q}$ are unitary, the lengths $\mathcal{M}_n$ of the receive vectors $\mathbf{d}_n$ are typically less than 1 due to the cross-correlations among receive elementary Hermites. Since $\mathbf{X}$ is upper-triangular, the higher the order of the orthogonalized combined pulse $\xi_n(t)$, the larger the number of elementary orthogonal Hermite pulses needed to compose it and the lower the length $\mathcal{M}_n$ of its corresponding receive vector $\mathbf{d}_n$. In other words, the probability of error associated to an orthogonalized pulse $\xi_n(t)$ increases with n. This impacts on the performance of higher order PSM schemes based on the orthogonal design presented here.

The length of a receive vector is, therefore, a measure of its distance to the noise subspace. Given that $d_n(t)$ is fully orthogonal to all other $d_m(t)$ $(m \neq n)$, the quantity $\mathcal{M}_n$ is an indication of the *isolation* of $d_n(t)$ from both the noise and interference subspaces and is therefore hereafter referred to as the *isolation coefficient*.

Fig. 6 shows how the isolation of $d_n(t)$ decreases with n in designs using 4 and 8 elementary Hermites, respectively. The

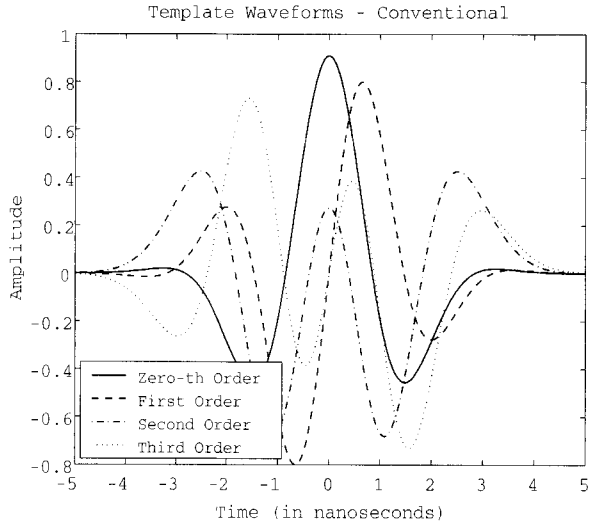

Fig. 7. Template waveforms obtained with proposed orthogonal design using conventional Hermite pulses as elementary components.

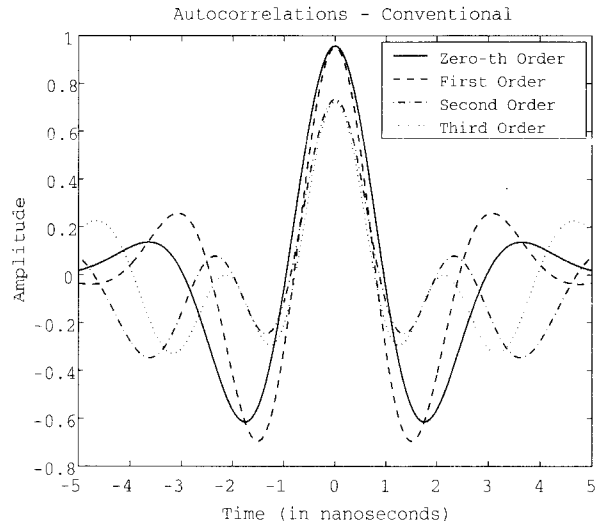

Fig. 8. Pseudo auto-correlation of the orthogonalized receive pulses obtained with proposed orthogonal design using the conventional Hermite pulses as elementary components.

plot shows results obtained with both matched and non-matched banks of correlators at the receiver.

In the next subsections, it is shown that the orthogonalization procedure introduced here can be understood as a kind of pulse-shape design that is robust against the distortion introduced by differentiating antennas.

D. Alternative Interpretation

The signal processing that occurs at the receiver within the proposed orthogonal design can be interpreted (or implemented) in the following alternative way. Given that the transmitter generates the waveforms $\xi_n(t)$ defined in (37), the respective receive waveforms are $\theta_n(t)$, given in (41). These receive waveforms are compared against normalized templates constructed as in (37), but using the entries of $\mathbf{Q}$ as coefficients, giving

$$\vartheta_m(t) = \mathcal{Y}_m \sum_{n=0}^{N-1} q_{n,m}\psi_n(t), \tag{45}$$

where the normalization coefficient $\mathcal{Y}_n$ is simply

$$\mathcal{Y}_m = \sqrt{\left(\sum_{n=0}^{N-1} q_{n,m}\right)^2}. \tag{46}$$

This indicates that the proposed orthogonal design has an additional advantage of not requiring the knowledge of whether pulses arrive inverted or not at the receiver. Indeed, since all received vector are orthogonalized by the design performed on the transmit pulses, only the magnitude of the projections of a received noisy (distorted) vector onto the basis of possible orthogonal vectors is relevant in detection. In other words, coherent-like performance is achievable with a non-coherent-like detection scheme.

Fig. 7 shows the four waveforms obtained using (45) for $N = 4$. Although not matched to the second derivatives of the waveforms given by (37) (effectively received pulses), these template waveforms form an orthonormal basis of the N-dimensional Hermite space which is rotated so as to be closest to the non-orthogonal basis given by the receive waveforms. In other words, the correlations between $\theta_n(t)$ and $\vartheta_n(t)$ are maximized for all n, while those between $\theta_n(t)$ and $\vartheta_m(t)$ are ensured to be zero.

Consider the correlation function

$$R_{\theta_n\vartheta_m}(\tau) = \int_{-\infty}^{\infty} \theta(t)\vartheta_m(t-\tau)dt. \tag{47}$$

Although $\theta_n(t)$ and $\vartheta_n(t)$ are clearly not the same waveforms, we refer to $R_{\theta_n\vartheta_n}(\tau)$ as the *pseudo* auto-correlation function of the orthogonalized receive pulse of order n. Fig. 8 shows the plots of these pseudo auto-correlation functions corresponding to the waveforms shown in Figs. 5 and 7.

It is noticeable that the peaks of the curves shown in Fig. 8 are not unitary. Indeed, these peak values are given by $\mathcal{M}_n$ and their distribution across the order of the corresponding pulses is the same as that of the diagonal values of $\mathbf{D} \cdot \mathbf{Q}$, where $\mathbf{D}$ is a matrix whose columns are given by $\mathbf{d_n}$, with $n = 1, \cdots, N$. As pointed out in Section II, the performance of a pulse-shape modulated ultra-wideband system using these pulses in the presence of additive white Gaussian noise will be determined by how close this distribution is to a unitary uniform distribution.

Analogously, we refer to $R_{\theta_n\vartheta_m}(\tau)$ as the *pseudo* cross-correlation function of the orthogonalized receive pulses of orders n and m. In the presence of jitter, the performance of a pulse-shape modulated ultra-wideband system using these pulses will depend on the behavior of the pseudo auto-correlation and cross-correlation functions in the vicinity of the origin.

Fig. 9 shows the envelope of the pseudo cross-correlation functions corresponding to the waveforms shown in Figs. 5 and 7.

Figs. 8 and 9 show that the pulses obtained with the proposed design, in addition to being orthogonal, exhibit similar corre-

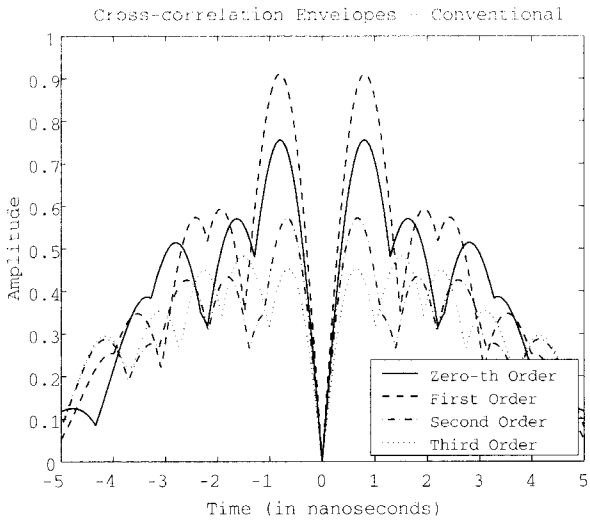

Fig. 9. Pseudo cross-correlation of the orthogonalized receive pulses obtained with proposed orthogonal design using the conventional Hermite pulses as elementary components.

lation properties regardless of the pulse order. This is in contrast to that observed with conventional Hermite pulses, whose auto- and cross-correlation properties degrade with the pulse order [1]. From an information-theoretical point of view, it can therefore be said that the proposed orthogonal design is a type of analog source-encoder that increases the entropy of the waveform alphabet used in the PSM scheme.

In the next subsection, the performance of M-ary PSM schemes based on the design introduced here is analyzed through computer simulations.

E. Performance of Orthogonalized PSM

The bit error rate performances of 4-ary pulse-shape modulated ultra-wideband systems with coherent detection are compared to the proposed orthogonalized scheme in Fig. 10. Since it was shown in Figs. 2 and 3 that PSM systems with conventional Hermites perform better when coherent detection is applied, the curves for non-coherent schemes have been omitted.

Fig. 10 clearly shows that the proposed orthogonalization method significantly enhances the performance of vector-based M-ary PSM systems. The improvement attained with the proposed design method derives from the fact that receive vectors corresponding to the designed transmit waveforms are orthogonal. In contrast, with conventional Hermite pulses, though coherent detection is better than non-coherent, it is performed over non-orthogonal receive vectors (see III-C and III-D).

Fig. 6, nevertheless, indicates that the performance of higher order pulse-shape modulation schemes still degrade with the order, despite the enhancement achieved with the orthogonal design. This is further illustrated in Fig. 11 which compares the bit error rate performances of 4-ary and 8-ary pulse-shape modulated ultra-wideband systems with matched receiver and coherent detection to that of the proposed orthogonalized scheme.

It is seen that the performance of the pulse-shape modulation scheme with the orthogonal design utilizing conventional Hermite pulses still degrades as the order increases. In the next

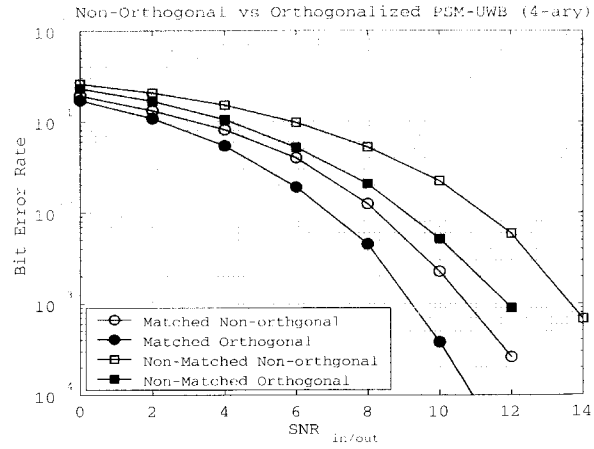

Fig. 10. Bit error rate performances of 4-ary pulse-shape modulated ultra-wideband systems. Curves for coherent detection schemes are compared to the proposed orthogonalized scheme with matched and non-matched receivers.

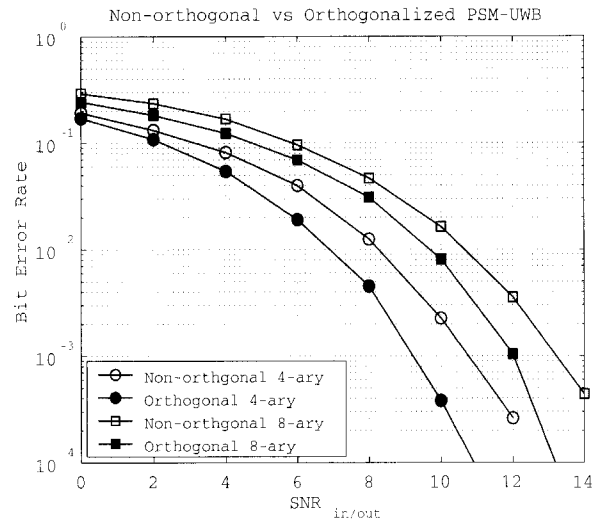

Fig. 11. Bit error rate performances of 4-ary and 8-ary pulse-shape modulated ultra-wideband systems. Curves for the matched receiver with coherent detection and of the proposed orthogonalized scheme are shown.

section, a new set of elementary pulses also constructed based on the Hermite polynomials is proposed, which further enhances the performance of PSM systems with the orthogonal design introduced here.

V. PROPOSED SET OF ELEMENTARY PULSES

A. Definition

The analysis in Section III showed that an undesired consequence of choosing $a = 2$ in (12) is that the elementary Hermite pulses arriving at the receiver are not in the same set as the generated pulses. It was also shown that if the same set of waveform generators used for transmission are utilized for reception (non-matched receiver), a significant amount of the transmit energy is not utilized in the detection process. On the other hand, if pulses cannot be integrated at the receiver prior to correlation, a

set of waveform generators distinct to that used at transmission is necessary at reception.

These are the matched and non-matched receiver structures discussed in Sections III-C and III-D. It was shown in Sections III-E and IV-E that PSM schemes with matched receivers outperform those with non-matched receivers, at the cost of requiring distinct waveform generators for transmission and reception.

Consider, however, the following set of Hermite pulses defined making $a = 1$ in (12), yielding

$$\rho_n(t) = \mathcal{U}_n e^{-t^2} H_n(t). \tag{48}$$

The normalization factor for these pulses can be computed from the following known property of Hermite polynomials [14]:

$$\int_{-\infty}^{\infty} e^{-2t^2} H_n^2(t)dt = 2^{\left(n-\frac{1}{2}\right)}\Gamma\left(n+\tfrac{1}{2}\right). \tag{49}$$

This gives

$$\mathcal{U}_n = \left(\sqrt{2^{\left(n-\frac{1}{2}\right)}\Gamma\left(n+\tfrac{1}{2}\right)}\right)^{-1}. \tag{50}$$

Using (11a) and (11b) it is easy to see that the m-th derivative of the n-th order pulse is given by:

$$\rho_n^{(m)}(t) = (-1)^m \frac{\mathcal{U}_n}{\mathcal{U}_{n+m}} \rho_{n+m}(t). \tag{51}$$

Equation (51) indicates that, unlike the set of orthogonal Hermite pulses, this set of pulses is closed with respect to differentiation, i.e.), derivatives of a given pulse are in fact just scaled versions of higher order pulses in the same set. In other words, with this pulse set, a receive matched bank of correlators can be constructed using the same set of waveforms utilized at the transmit bank of pulse generators.

B. Properties

The cross-correlation of the waveforms given in (48) can then be written as

$$R_\rho(n,m) = \mathcal{U}_n \mathcal{U}_m K(n,m), \tag{52}$$

where the auxiliary function $K(n,m)$ is a generalization of (49) to the case when $n \neq m$ and is given by (67) in the appendix.

From (51), the cross-correlation of the k-th derivative of the waveforms defined by (48) is simply given by

$$\begin{aligned} R_{\rho^{(k)}}(n,m) &= \int_{-\infty}^{\infty} \rho_n^{(k)}(t)\rho_m^{(k)}(t)dt = \mathcal{U}_n\mathcal{U}_m K(n+k,m+k) \\ &= \frac{K(n+k,m+k)}{\sqrt{2^{(n+m-1)}\Gamma\left(n+\frac{1}{2}\right)\Gamma\left(m+\frac{1}{2}\right)}}. \end{aligned} \tag{53}$$

It is clear from (52) and (67) that $K(n,n)$ is always positive and $R_\rho(n,n) = 1$, which gives

$$\mathcal{U}_n = \frac{1}{\sqrt{K(n,n)}}. \tag{54}$$

Table 3. Correlation property of proposed pulse set.

$a=1$		Order of $\rho_m(t)$							
		0	1	2	3	4	5	6	7
Order of $\rho_{n+2}(t)$	2	−0.577	0	1	0	−0.845	0	0.595	0
	3	0	−0.775	0	1	0	−0.882	0	0.664
	4	0.293	0	−0.845	0	1	0	−0.905	0
	5	0	0.488	0	−0.882	0	1	0	−0.920
	6	−0.147	0	0.595	0	−0.905	0	1	0
	7	0	−0.286	0	0.664	0	−0.920	0	1
	8	0.074	0	−0.383	0	0.712	0	−0.931	0
	9	0	0.161	0	−0.457	0	0.749	0	−0.940

Following the same procedure as that of Section III-B, the efficiency coefficient for the transmit antennas is obtained by substituting (51) into (53), giving

$$\eta_{\text{TX}}(n) = \frac{1}{\sqrt{R_{\rho'}(n,n)}} = \frac{\mathcal{U}_{n+1}}{\mathcal{U}_n}. \tag{55}$$

The n-th order elementary transmit waveform is then be given by

$$\eta_{\text{TX}}(n)\rho_n'(t) = -\rho_{n+1}(t). \tag{56}$$

Similarly, the efficiency coefficient of the receive antenna is given by

$$\eta_{\text{RX}}(n) = \frac{\mathcal{U}_{n+2}}{\mathcal{U}_{n+1}}. \tag{57}$$

Consequently, the output of the an efficient differentiating receive antenna becomes

$$-\eta_{\text{TX}}(n)\rho_{n+1}'(t) = \rho_{n+2}(t). \tag{58}$$

From (56) and (58), it is seen that with this set of pulses, the output of an efficient antenna to an n-th order pulse is simply an $n+1$ order pulse. In other words, if the n-th order pulse is generated at the transmitter, the corresponding receive pulse is given by an $n+2$ order pulse. As a result, a matched bank of correlators can be constructed using the same set of pulses used for transmission.

Indeed, consider a bank of correlators that compares the received waveforms with templates taken from the same set of pulses used at transmission. The output of such a bank of correlators is given by

$$\int_{-\infty}^{\infty} \rho_{n+2}(t)\rho_m(t)dt = R_\rho(n+2,m). \tag{59}$$

Table 3 gives a few numeric values of (59). It is clearly seen from the table that the second (positive) diagonal of this cross-correlation matrix is unitary. As it is known that it is impossible to receive 0-th or 1-st order pulses (unless integration is used), all that it takes to obtain a matched bank of correlators is to remove the first two columns and add two others of orders N and $N+1$.

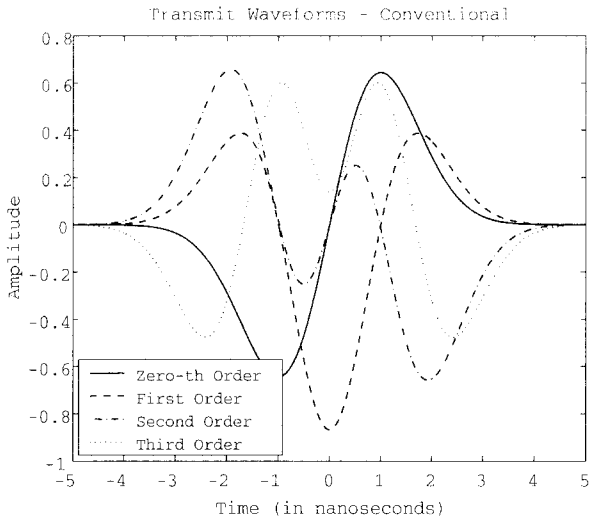

Fig. 12. Transmit waveforms obtained with proposed orthogonal design using the proposed Hermite pulses as elementary components.

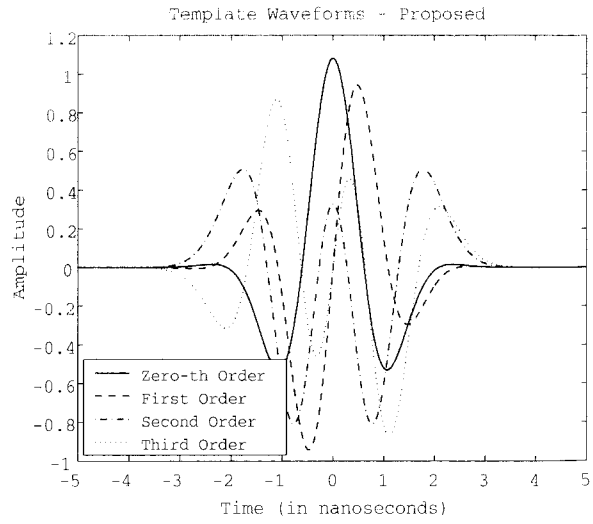

Fig. 13. Template waveforms obtained with proposed orthogonal design using the proposed Hermite pulses as elementary components.

The burden associated with a matched receiver is therefore significantly less than that of a system using conventional Hermite pulses. Unlike the latter, where two completely distinct sets of waveform generators are required, here only two of all waveform generators available at the transceivers are not used at transmission (N and $N+1$) or at reception (0 and 1).

Comparing the last $N-3$ columns of Table 3 to the first $N-3$ columns of Table 1, it is also evident that the lengths of the output vectors of a matched receiver using the proposed pulse set are larger than those using the set of conventional Hermite pulses. This suggests that the orthogonalization method introduced in Section IV will perform better with the proposed set of pulses.

Let us now consider the use of these pulses as elementary Hermites in the orthogonal design presented in Section IV.

The entries of the distortion matrix $\mathbf{C}$ modeling this system are given by

$$c_{n,m} = R_\rho(n+2, m+2). \tag{60}$$

The orthogonalized m-th order generated, transmit, receive and template waveforms obtained using this new set of elementary pulses, equivalent to (37), (38), (41), and (45) are respectively given by

$$\xi_m(t) = \mathcal{M}_m \sum_{n=0}^{N-1} x_{n,m}\rho_n(t), \tag{61a}$$

$$\zeta_m(t) = -\mathcal{M}_m \sum_{n=0}^{N-1} x_{n,m}\rho_{n+1}(t), \tag{61b}$$

$$\theta_m(t) = \mathcal{M}_m \sum_{n=0}^{N-1} x_{n,m}\rho_{n+2}(t), \tag{61c}$$

$$\vartheta_m(t) = \mathcal{M}_m \sum_{n=0}^{N-1} q_{n,m}\rho_{n+2}(t). \tag{61d}$$

The transmit pulses obtained with $N=4$ and the corresponding template waveforms are shown in Figs. 12 and 13, respectively.

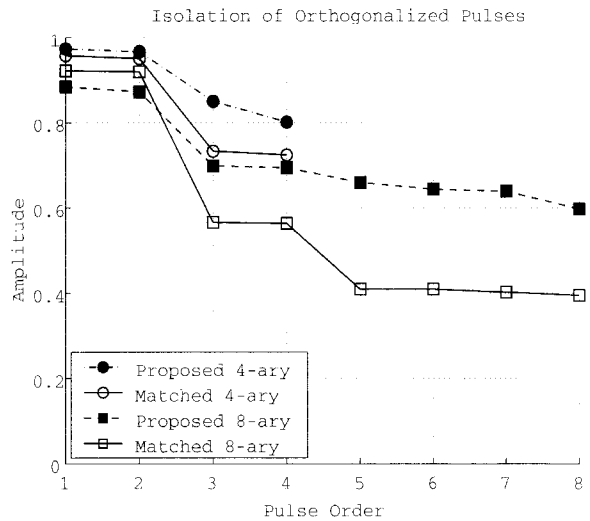

Fig. 14. Isolation coefficients of orthogonalized proposed and conventional Hermite pulses

Fig. 14 compares the isolation of the orthogonally designed Hermite-based receive vectors using the proposed set of elementary pulses against that achieved using conventional elementary Hermites [1].

It is seen from the plot that with the new pulse set, even the minimum isolation of the orthogonalized proposed pulses is around 0.6. In other words, in the worst case, about 60% of the energy of the receive pulse is effectively used in the detection process. This is in contrast with only 40% utilized when conventional elementary Hermites are used (higher order pulses).

The enhancement provided by using this new pulse set as elementary Hermites can also be appreciated by looking at the pseudo auto- and cross-correlation properties of the orthogonalized pulses, as was done in Section IV for conventional pulses. For the pulses shown in Fig. 12 and 13, these functions are

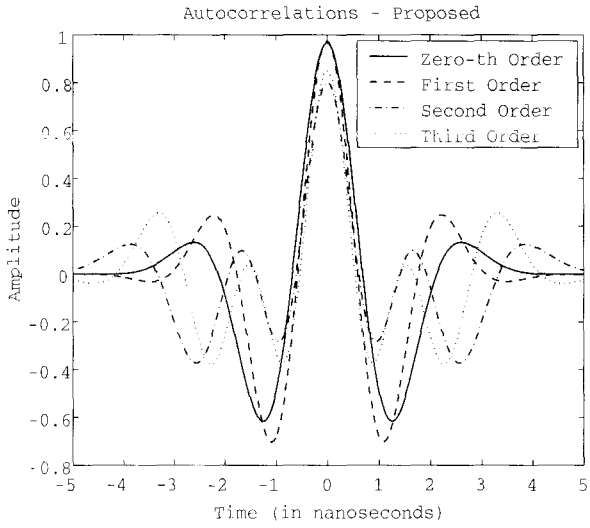

Fig. 15. Pseudo auto-correlations of the orthogonalized receive pulses obtained with proposed orthogonal design using the proposed Hermite pulses as elementary components.

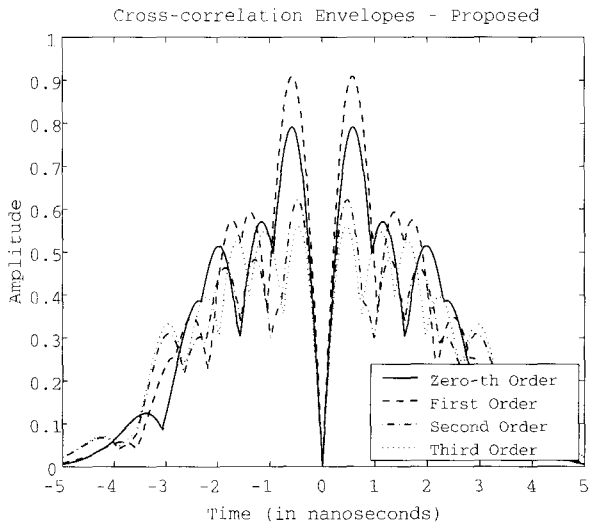

Fig. 16. Pseudo cross-correlations of the orthogonalized receive pulses obtained with proposed orthogonal design using the proposed Hermite pulses as elementary components.

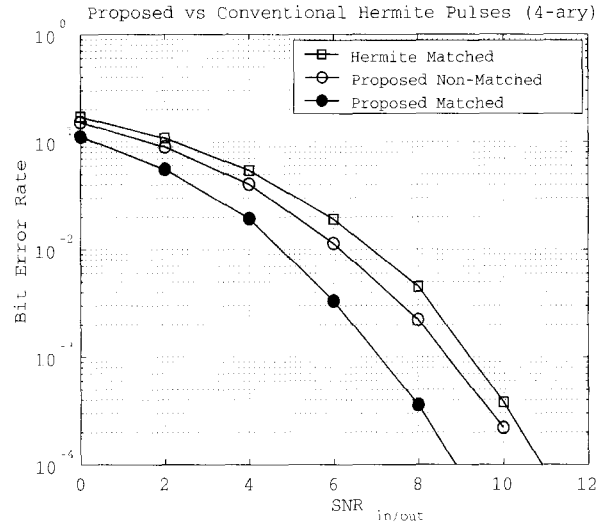

Fig. 17. Bit error rate of pulse-shape modulated ultra-wideband systems with orthogonalized waveforms. Curves for a 4-ary PSM scheme using conventional Hermites (matched correlators) and the proposed pulses (non-matched and matched correlators) are given.

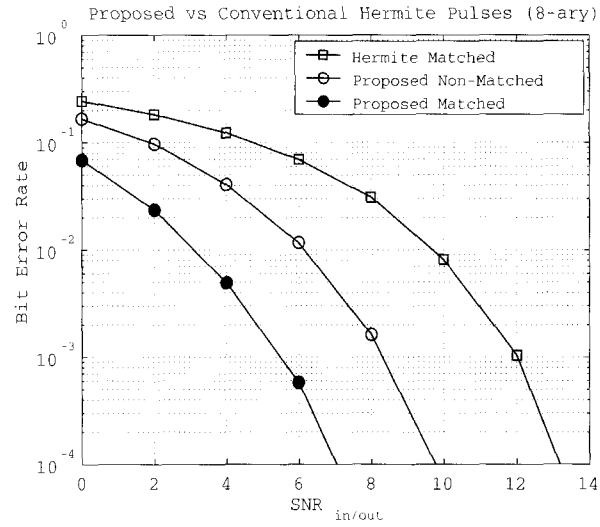

Fig. 18. Bit error rate of pulse-shape modulated ultra-wideband systems with orthogonalized waveforms. Curves for an 8-ary PSM scheme using conventional Hermites (matched correlators) and the proposed pulses (non-matched and matched correlators) are given.

shown in Fig. 15 and 16.

Comparing Figs. 8 and 15, it is seen that with the new set of elementary Hermites, better autocorrelation properties are obtained for the orthogonalized pulses, i.e., the peaks of all autocorrelation functions are closer to 1. This is in accordance with the results displayed in Fig. 14.

In the next subsection, the bit error rate performances of pulse-shape modulated ultra-wideband systems using the proposed orthogonal design and this new set of elementary pulses are compared to those using conventional Hermites.

C. Performance of Orthogonal PSM with Proposed Pulses

Fig. 17 shows the bit error rate performances of a 4-ary pulse-shape modulated ultra-wideband system with waveforms constructed using the proposed orthogonal design. The curve obtained using the conventional elementary Hermite pulses given by (14) and a matched bank of correlators is compared to those obtained using the proposed elementary pulses given by (48) with matched and non-matched banks of correlators.

The plot clearly shows that using the proposed set of elementary Hermite pulses significantly enhances the performance of the vector-based pulse-shape modulation scheme utilizing the proposed orthogonal design. Even with a non-matched bank of correlators, at a 10^{-3} error rate, a gain of about 0.5 dB is attained over the scheme using conventional Hermite pulses and a matched bank of correlators. Further, with a matched receiver, the scheme with the proposed pulse set outperforms the equivalent scheme using conventional Hermites by more than 2 dBs at a 10^{-3} error rate.

We emphasize that the scheme with matched correlators using conventional Hermites requires a complete additional set of waveform generators, unlike the proposed scheme which requires only two additional waveform generators belonging to the same set.

The gain obtained with the proposed design using the proposed set of Hermites is even larger in a higher order M-ary pulse-shape modulation scheme. This is illustrated in Fig. 18, which is the equivalent of Fig. 17 for an 8-ary pulse-shape modulated ultra-wideband system.

In 8-ary PSM, it is further seen that even with a non-matched bank of correlators, the orthogonalized PSM scheme using the proposed set of pulses gains almost 4 dB compared to the same system using conventional elementary Hermites and a matched receiver. This gain increases beyond 6 dBs if the system with the proposed pulse set also uses matched receivers. Finally, comparing Figs. 17 and 18, it is also seen that the proposed orthogonal design yields better performance with the higher order 8-ary scheme if the set of proposed pulses are used as elementary waveforms. This is unlike the observed when conventional Hermites are used as elementary waveforms.

VI. CONCLUSIONS

In this paper, it was shown that the application of Hermite polynomial-based waveforms to pulse-shape modulation schemes for ultra-wideband communications is not as straightforward as suggested in the current literature. It was established that Hermite pulses, while orthogonal when generated, lose their orthogonality at the receiver if the distortive effect of antennas are taken into account. The specific case of differentiating behavior which is typical of commonly found resistive-capacitive antennas was analyzed in detail.

The mathematical model of such distortion was used to derive a novel algebraic model for PSM-UWB-IR systems employing Hermite pulses. In order to overcome the problem of loss of orthogonality due to differentiating antennas, a new PSM scheme based on the Gram-Schmidt orthogonalization procedure was proposed. It was shown that this method can be understood as a type of analog code that orthogonalizes receive vectors and maximizes the entropy of the alphabet represented by their ensemble. Alternatively, the method can also be understood as a design that yields pulses with better auto- and cross-correlation properties than conventional Hermites in the presence of differentiating antennas.

A new set of elementary waveforms derived from the Hermite polynomial was further proposed, which improves the performance of the orthogonal design compared to that utilizing conventional Hermite pulses. The proposed pulses have the additional advantageous property that their derivatives fall in the same set. This enables the use of the same set of pulse generators at both transmission and reception.

The combination of these two proposed techniques enables the design of high-performance orthogonal PSM systems with simple hardware implementation.

Several simulation results are given which clearly illustrate the improvement achieved with the new orthogonal design and elementary pulse set over known PSM-UWB-IR schemes.

Although only differentiating distortion was considered, it is evident that the orthogonal design proposed can easily be extended to combat other types of distortion, provided that their mathematical models are known. For instance, some recent works suggest that the UWB channel may in fact act as an integrator in itself [25], [26]. If these results are proven right, the extension of the theory here presented is rather straightforward since the characterization of a first-order differentiating channel is included.

Finally, although only pulse-shape modulation was considered in this work, the theory presented can clearly be applied to more general combined pulse-shape and pulse-position modulation (PS-PPM) schemes such as discussed in [7].

APPENDIX

Without loss of generality let m be the larger and n the smaller between m and N:

$$D(n,m) = \int_{-\infty}^{\infty} e^{-t^2} H_n(t) H_m(t) dt = \begin{cases} 0 & \text{if } n \neq m \\ 2^n n! \sqrt{\pi} & \text{if } n = m, \end{cases} \tag{62}$$

$$E(n,m) = \int_{-\infty}^{\infty} t e^{-t^2} H_n(t) H_m(t) dt = \begin{cases} 2^n m! \sqrt{\pi} & \text{if } m - n = 1 \\ 0 & \text{otherwise,} \end{cases} \tag{63}$$

$$F(n,m) = \int_{-\infty}^{\infty} t^2 e^{-t^2} H_n(t) H_m(t) dt = \begin{cases} \left(n + \frac{1}{2}\right) 2^n n! \sqrt{\pi} & \text{if } n = m \\ 2^n m! \sqrt{\pi} & \text{if } m - n = 2 \\ 0 & \text{otherwise,} \end{cases} \tag{64}$$

$$G(n,m) = \int_{-\infty}^{\infty} t^4 e^{-t^2} H_n(t) H_m(t) dt = \begin{cases} \left(\frac{3}{2}n^2 + \frac{3}{2}n + \frac{3}{4}\right) 2^n n! \sqrt{\pi} & \text{if } n = m \\ (n + m + 1)\, 2^n m! \sqrt{\pi} & \text{if } m - n = 2 \\ 2^n m! \sqrt{\pi} & \text{if } m - n = 4 \\ 0 & \text{otherwise,} \end{cases} \tag{65}$$

$$K(n,m) = \int_{-\infty}^{\infty} e^{-2t^2} H_n(t) H_m(t) dt = \begin{cases} 0 & \text{if } mod(n+m,2) \neq 0 \\ (-1)^{\frac{m-n}{2}} 2^{\frac{n+m-1}{2}} \Gamma\left(\frac{n+m+1}{2}\right) & \text{otherwise,} \end{cases} \tag{66}$$

where $mod(a,b)$ denotes the modulus operation between a and b and $\Gamma()$ is the Gamma function.

REFERENCES

[1] M. Ghavami, L. B. Michael, and R. Kohno, "A novel UWB pulse shape modulation system," *Kluwer Int. J. Wireless Pers. Commun.*, vol. 23, no. 1, pp. 105–120, Aug. 2002.

[2] S. Ciolino, M. Ghavami, and H. Aghvami, "UWB pulse shape modulation system using wavelet packets," in *Proc. IWUWBS'03*, Oulu, Finland, June 2003.
[3] M. Pinchas and B. Z. Bobrovsky, "Orthogonal laguerre polynomial pulses for ultra-wideband communications," in *Proc. IWUWBS'03*, Oulu, Finland, June 2003.
[4] L. B. Michael, M. Ghavami, and R. Kohno, "Multiple pulse generator for ultra-wideband communicaitons using hermite polynomial based orthogonal pulses," in *Proc. IEEE Conf. Ultra Wideband Sys. Technol.*, Baltimore, U.S.A., May 2002, pp. 47–51.
[5] J. A. N. da Silva and M. L. R. de Campos, "Orthogonal pulse shape modulation for impulse radio," in *Proc. ITS'02*, Natal, Brazil, Sept. 2002, pp. 916–921.
[6] M. Z. Win and R. A. Scholtz, "Impulse radio: How it works," *IEEE Commun. Lett.*, vol. 2, pp. 36–38, 1998.
[7] C. J. Mitchell, G. T. F. de Abreu, and R. Kohno, "Combined pulse shape and pulse position modulation for high data rate transmissions in uwb communications," *Int. J. Wireless Information Network - Special Issue on UWB (to appear)*, vol. 11, Apr. 2004.
[8] T. P. Montoya and G. S. Smith, "A study of pulse radiation from several broad-band loaded monopoles," *IEEE Trans. Antennas Propagat.*, vol. 44, no. 8, pp. 1172–1182, Aug. 1996.
[9] Y. T. Lo and S. W. Lee, *Antenna Handbook - Theory, Applications and Design*, Van Nostrand Reinhold, 1988.
[10] C. J. Mitchell, G. T. F. de Abreu, and R. Kohno, "Two dimensional codulation for uwb systems," in *Proc. ISITA'02*, vol. I, Ikaho, Gunma, Japan, Dec. 2002, pp. 307–310.
[11] J. G. Proakis, *Digital Communications*, fourth edition, New York, NY: Mc-Graw-Hill, 2000.
[12] F. M. Reza, *An Introduction to Information Theory*, New York, NY: Dover, 1994.
[13] A. D. Poularikas, *The Transforms and Applications Handbookf* , second edition, CRC Press, Feb.23 2000.
[14] I. S. Gradshteyn and I. M. Ryzhik, *Table of Integrals, Series, and Products*, sixth edition, Academic Press, July 2000.
[15] G. T. F. de Abreu, C. J. Mitchell, L. G. F. Trichard, and R. Kohno, "A note on the application of hermite pulses in uwb communications," in *Proc. IWUWBS'03*, Oulu, Finland, June 2003.
[16] M. Z. Win and R. A. Scholtz, "Ultra-wide bandwidth time-hopping spread-spectrum impulse radio for wireless multiple-access communications," *IEEE Trans. Commun.*, vol. 48, no. 4, pp. 679–691, Apr. 2000.
[17] M. Z. Win and R. A. Scholtz, "Ultra-wide bandwidth signal propagation for indoor wireless communications," in *Proc. ICC'97*, Montréal, Canada, June 1997, pp. 56–60.
[18] G. T. F. de Abreu and R. Kohno, "Design of jitter-robust orthogonal pulses for UWB systems," to appear in *Proc. Globecomm'03*, San Francisco, U.S.A., Dec. 2003.
[19] G. T. F. de Abreu and R. Kohno, "Jitter robust hermite pulses for uwb communications," in *Proc. ISITA'02*, Awajishima, Japan, Dec. 15-18, 2003.
[20] M. Z. Win and R. A. Scholtz, "Characterization of ultra-wide bandwidth wireless indoor channels: A communication-theoretic view," *IEEE J. Select. Areas Commun.*, vol. 20, no. 9, pp. 1613–1627, Dec. 2002.
[21] A. Álvarez *et al.*, "Ultrawideband channel characterization and modelling," in *Proc. IWUWBS'03*, Oulu, Finland, June 2-5, 2003.
[22] J. Keignart and N. Daniele, "Channel sounding and modelling for indoor uwb communications," in *Proc. IWUWBS'03*, Oulu, Finland, June 2-5, 2003.
[23] T. Sato, G. T. F. de Abreu, and R. Kohno, "Beamforming array antenna with heterogeneous signal distribution for uwb pulse transmission," *IEICE Trans. Fund. of Electronics, Commun. Comput. Sciences - Special Issue on Wideband Systems (to appear)*, Dec. 2003.
[24] G. H. Golub and C. F. van Loan, *Matrix Computations*, third edition, New York, NY: Johns Hopkins Univ. Press, Nov. 1996.
[25] A. Armogida *et al.*, "Path loss modelling in short-range uwb transmissions," in *Proc. IWUWBS'03*, Oulu, Finland, June 2003.
[26] C. Roblin, S. Bories, and A. Sibille, "Characterization tools of antennas in the time domain," in *Proc. IWUWBS'03*, Oulu, Finland, June 2-5 2003.

Giuseppe T. F. de Abreu was born in Salvador-Bahia, Brazil in December 1972. He received his B.E. in electronics engineering and a *Latus Sensu* degree of specialist in telecommunications, from the Federal University of Bahia - Brazil, in 1996 and 1997, respectively. In 2001 he received his M.E. in electrical and computer engineering from the Yokohama National University - Japan and is scheduled to be awarded his Ph.D. degree from the same institution in March, 2004. His research interests are spatial and temporal signal processing, smart antennas, beamforming, space-time coding, and ultra-wideband systems. He was the recipient of the *Uenohara Foreign Student's Award for Excellence in Research* from Tokyo University in 2000. Giuseppe Abreu has authored/co-authored 2 registered patents and various international conference and journal papers.

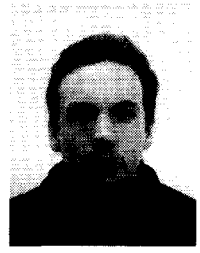

Craig J. Mitchell was born in Johannesburg, South Africa in November 1975. He received both his B.Sc. (*summa cum laude*) and M.Sc. in electrical engineering from the University of the Witwatersrand - South Africa in 1997 and 2001, respectively. He is currently working towards his Ph.D. at the Yokohama National University - Japan. His research interests lie in the areas of ultra-wideband systems, coding wireless communications.

Ryuji Kohno was born in Kyoto, Japan in March 1956. He received his B.E. and M.E. degrees in computer engineering from Yokohama National University in 1979 and 1981, respectively, and Ph.D. degree in electrical engineering from the University of Tokyo in 1984. He joined the Department of Electrical Engineering, Tokyo University, in 1984 and was made an Associate Professor in 1986. From 1988–1997 he was an Associate Professor in the Division of Electrical and Computer Engineering, Yokohama National University, where he is now a Full Professor. He is the Chairman of the Societies of ITS and Software Radio of the IEICE, an Editor to the IEEE Transactions on Communications and on Information Theory, and of the IEICE Transactions on Fundamentals of Electronics, Communications, and Computer Sciences. His research interests lie in several areas of wireless, optical and cable communications, coding and information theory, spread spectrum and ultra-wideband systems, etc. He is the author of several technical books and numerous papers.